



New antimicrobial terpenoids and phloroglucinol glucosides from *Syzygium szemaoense*

Wen Xu, Junfeng Tan, Yu Mu, Dan Zheng, Xueshi Huang*, Liya Li*

Institute of Microbial Pharmaceuticals, College of Life and Health Sciences, Northeastern University, Shenyang 110819, PR China

ARTICLE INFO

Keywords:

Syzygium szemaoense
Terpenoid
Phloroglucinol
Antimicrobial activity

ABSTRACT

Six new terpenoids (1–6) and two new phloroglucinol glucosides (7 and 8) were isolated from the extract of *Syzygium szemaoense* leaves. Among the isolates, compounds 1 and 2 (named syzygiumursanolides A and B) were unusual 28-norursane type triterpenoids with 19(18→17)-abeo spirocyclic skeleton. And syzygiumone B (8) was rare ascorbyl-modified phloroglucinol glucoside. Their structures were elucidated on the basis of comprehensive 1D and 2D NMR, HRESIMS spectroscopic data analysis, as well as experimental and calculated ECD spectra and acid hydrolysis. Antimicrobial bioassay revealed that syzygiumursanolide D (4) displayed the most potent antifungal activities with MIC values ranging from 6.25 to 25 µg/mL against a panel of fungi.

1. Introduction

The genus *Syzygium* (family: Myrtaceae), consisting of > 1200 species, are distributed in tropical and subtropical regions of the world [1]. Many species of this genus such as *S. Cordatum*, *S. samarangense*, *S. aromaticum* and *S. cumini* (syn. *Eugenia jambolana* Lam) are valuable medicinal plant used to treat cancer, fever, diarrhea, diabetes, etc. [2–5]. Some plants, including *S. aromaticum* and *S. cumini*, are also widely used in food and nutraceutical industry due to their high nutritional and health beneficial values [6,7]. Among reported multiple pharmacological activities of *Syzygium* spp., antimicrobial activities were noteworthy since many medicinal plants from *Syzygium* genus have been used in folk medicine to treat infection related disease, such as fever and diarrhea [3–5]. Terpenoids and phloroglucinols are important secondary metabolites present in plants of *Syzygium* genus. In recent years, more and more bioactive terpenoids with anticancer and antimicrobial activities, as well as phloroglucinol derivatives with cytotoxic, antioxidant and protein tyrosine phosphatase 1B inhibitory activities have been isolated and identified from *S. guineense* [8], *S. jambos* [9], *S. samarangense* [10], and *S. austroyunnanense* [11]. Our previous work on *S. cumini* also yielded 24 sesquiterpenoids [12], 14 triterpenoids [13], as well as 16 phloroglucinols [14]. Thus, the genus *Syzygium* is a good source for finding bioactive novel terpenoids and phloroglucinols.

S. szemaoense is a fruit tree distributed in southwest region of China. To date, no research on the chemical constituents and bioactivities of *S. szemaoense* have been reported. In our continuing search for bioactive

constituents from *Syzygium* genus, the extract of *S. szemaoense* collected in Yunnan, China was found possessing antimicrobial activities against a panel of bacterial and fungi *in vitro*. Further phytochemical study yielded six new terpenoids and two new phloroglucinol glucosides from the ethanol extract of *S. szemaoense* leaves. Among the isolates, compounds 1 and 2 contain unique 19(18→17)-abeo-28-norursane spirocyclic skeleton, and compound 8 is a tricyclic phloroglucinol glucoside with a novel carbon skeleton. Herein, we reported the isolation and structure elucidation of eight new compounds (1–8), as well as their antimicrobial activities *in vitro*. Meanwhile, hypothetical biogenetic pathway of compound 8, a novel ascorbyl-adduct phloroglucinol derivative, were also discussed and presented.

2. Experimental

2.1. General experimental procedures

Optical rotations were recorded on an Anton Paar MCP200 automatic polarimeter. IR spectra were measured with a Bruker Tensor 27 FT-IR spectrometer (film). 1D and 2D NMR spectra were collected on a Bruker Advance III-600 MHz spectrometer (Bruker Co., Rheinstetten, Germany) with deuterated dimethyl sulfoxide (DMSO-*d*₆) as solvents. ECD spectra was acquired from a Biologic MOS-450 spectropolarimeter (Biologic Science, Claix, France) at room temperature. HRESIMS were performed using a Bruker Micro TOF-Q mass spectrometer (Bruker Daltonics, Billerica, MA, USA), or a Shimadzu MALDI-TOF mass spectrometer (Shimadzu Corporation, Kyoto, Japan). GC-MS analyses were

* Corresponding authors.

E-mail addresses: huangxs@mail.neu.edu.cn (X. Huang), lyli@mail.neu.edu.cn (L. Li).

<https://doi.org/10.1016/j.bioorg.2020.104242>

Received 10 July 2020; Received in revised form 15 August 2020; Accepted 25 August 2020

Available online 28 August 2020

0045-2068/ © 2020 Elsevier Inc. All rights reserved.

Table 1
 ^1H NMR (600 MHz) and ^{13}C NMR (150 MHz) Data of Compounds 1–4 in DMSO- d_6 .

position	1		2		3		4	
	δ_{C} , type	δ_{H} (J in Hz)	δ_{C} , type	δ_{H} (J in Hz)	δ_{C} , type	δ_{H} (J in Hz)	δ_{C} , type	δ_{H} (J in Hz)
1	49.4 CH ₂	1.78 (m) 0.70 (t, 11.9)	49.3 CH ₂	1.84 (dd, 12.6, 4.8) 0.95 (m)	49.3 CH ₂	1.72 (dd, 12.0, 4.4) 0.71 (t, 12.0)	46.7 CH ₂	1.86 (m) 0.82 (m)
2	67.5 CH	3.53 (m)	71.6 CH	3.26 (m)	67.5 CH	3.51 (m)	66.4 CH	3.54 (m)
3	75.7 CH	3.11 (d, 9.5)	77.8 CH	3.50 (d, 8.7)	75.7 CH	3.10 (overlapped)	94.6 CH	2.84 (d, 9.0)
4	43.1 C		149.2 C		43.1 C		40.1 C	
5	46.4 CH	1.16 (s)	51.0 CH	1.60 (m)	46.5 CH	1.14 (s)	54.3 CH	0.80 (m)
6	65.8 CH	4.25 (overlapped)	67.5 CH	4.20 (br s)	65.8 CH	4.24 (br s)	18.0 CH ₂	1.48 (m) 1.33 (m)
7	40.6 CH ₂	1.60 (m) 1.48 (m)	40.1 CH ₂	1.60 (m) 1.60 (m)	40.1 CH ₂	1.58 (d, 12.2) 1.36 (d, 12.2)	32.6 CH ₂	1.45 (m) 1.27 (m)
8	38.1 C		38.5 C		38.4 C		39.7 C	
9	47.4 CH	1.39 (dd, 11.4, 4.8)	44.8 CH	1.49 (m)	47.5 CH	1.52 (m)	46.9 CH	1.48 (m)
10	36.8 C		37.3 C		36.8 C		37.1 C	
11	22.60 CH ₂	1.98 (m) 1.88 (m)	23.4 CH ₂	1.95 (m) 1.95 (m)	23.1 CH ₂	1.96 (m) 1.90 (m)	23.0 CH ₂	1.86 (m) 1.86 (m)
12	117.7 CH	5.66 (t, 3.0)	118.0 CH	5.69 (t, 1.8)	125.6 CH	5.21 (t, 3.6)	124.2 CH	5.12 (t, 3.2)
13	142.1 C		142.5 C		136.7 C		138.5 C	
14	43.4 C		43.8 C		42.3 C		41.7 C	
15	27.5 CH ₂	1.70 (m) 1.02 (m)	27.4 CH ₂	1.69 (m) 1.03 (m)	27.5 CH ₂	1.86 (m) 1.01 (dt, 14.2, 4.0)	27.6 CH ₂	1.81 (m) 0.97 (m)
16	33.6 CH ₂	1.60 (m) 1.06 (m)	33.6 CH ₂	1.60 (m) 1.08 (m)	23.9 CH ₂	2.18 (m) 1.74 (m)	23.9 CH ₂	1.90 (m) 1.51 (m)
17	49.6 C		49.7 C		47.5 C		46.8 C	
18	70.8 CH	3.93 (m)	70.7 CH	3.93 (m)	54.6 CH	2.17 (overlapped)	52.5 CH	2.12 (d, 10.8)
19	54.0 CH	0.85 (m)	54.0 CH	0.86 (m)	36.6 CH	2.37 (m)	38.5 CH	1.27 (m)
20	40.5 CH	1.78 (m)	40.5 CH	1.78 (m)	152.8 C		38.6 CH	0.92 (m)
21	33.2 CH ₂	1.70 (m) 0.93 (m)	33.2 CH ₂	1.69 (m) 0.92 (m)	33.6 CH ₂	2.29 (m) 2.15 (m)	30.3 CH ₂	1.42 (m) 1.27 (m)
22	27.1 CH ₂	1.48 (m) 1.12 (m)	27.1 CH ₂	1.49 (m) 1.15 (m)	38.0 CH ₂	1.79 (dt, 9.6, 6.4) 1.48 (m)	36.4 CH ₂	1.55 (m) 1.27 (m)
23	63.7 CH ₂	3.38 (overlapped) 3.19 (d, 10.4)	106.4 CH ₂	5.35 (s) 5.21 (s)	63.7 CH ₂	3.37 (dd, 10.8, 4.8) 3.20 (overlapped)	28.7 CH ₃	0.92 (s)
24	15.0 CH ₃	0.91 (s)			15.0 CH ₃	0.90 (s)	17.8 CH ₃	0.74 (s)
25	18.7 CH ₃	1.32 (s)	17.8 CH ₃	1.00 (s)	18.3 CH ₃	1.28 (s)	16.3 CH ₃	0.92 (s)
26	19.0 CH ₃	1.07 (s)	19.7 CH ₃	1.13 (s)	18.2 CH ₃	0.96 (s)	17.0 CH ₃	0.74 (s)
27	22.62 CH ₃	0.99 (s)	22.3 CH ₃	1.03 (s)	23.1 CH ₃	1.05 (s)	23.3 CH ₃	1.04 (s)
28					174.4C		178.6C	
29	11.5 CH ₃	0.98 (d, 7.2)	11.6 CH ₃	0.99 (d, 7.2)	16.1 CH ₃	0.95 (d, 6.6)	17.1 CH ₃	0.82 (d, 6.0)
30	19.2 CH ₃	0.84 (d, 6.6)	19.2 CH ₃	0.84 (d, 6.6)	104.8 CH ₂	4.67 (br s) 4.58 (br s)	21.2 CH ₂	0.91 (d, 6.0)
1'					94.3 CH	5.18 (d, 8.2)	103.3 CH	4.63 (br s)
2'					72.3 CH	3.08 (m)	70.8 CH	3.73 (br s)
3'					77.6 CH	3.13 (m)	70.5 CH	3.46 (dd, 9.6, 3.0)
4'					69.6 CH	3.12 (m)	71.8 CH	3.23 (t, 9.6)
5'					76.6 CH	3.20 (m)	69.4 CH	3.68 (dt, 9.6, 6.1)
6'					60.7 CH ₂	3.58 (dd, 10.2, 5.4) 3.44 (m)	17.8 CH ₃	1.12 (d, 6.0)
OH-2		4.21 (br s)		4.56 (br s)		4.17 (d, 4.2)		4.18 (br s)
OH-3		4.11 (br s)		4.81 (br s)		4.07 (d, 4.2)		
OH-6		4.05 (d, 3.6)		4.20 (br s)		4.05 (d, 4.2)		
OH-18		4.24 (d, 6.1)		4.25 (d, 6.0)				
OH-23		4.33 (br s)				4.31 (t, 5.4)		

conducted on a Shimadzu GCMS-QP2020 gas chromatograph mass spectrometer equipped with an AOC-20i auto injector (Shimadzu Corporation). Silica gel (100–200 mesh, 300–400 mesh, Qingdao Marine Chemical Ltd., Qingdao, China), Sephadex LH-20 (GE Healthcare Bio-sciences AB, Uppsala, Sweden), MCI gel (CHP-20P, Mitsubishi Chemical Corporation, Tokyo, Japan), ODS-A (S-50 μm , 12 nm, YMC Co., Ltd, Kyoto, Japan) were used for column chromatography. Unless otherwise specified, all chemicals and solvents were purchased from Sinopharm Chemical Reagent Co., Ltd. (Shenyang, People's Republic of China).

2.2. Plant material

The leaves of *S. szemaense* were collected in September 2017 from Si Mao city, Yunnan Province, People's Republic of China, and were

identified by Professor Guodong Li, Yunnan University of Traditional Chinese Medicine. A voucher specimen (zf0089) has been deposited at the Institute of Microbial Pharmaceuticals, Northeastern University, Shenyang, China.

2.3. Extraction and isolation

The dried leaves powder of *S. szemaense* (5.0 kg) were successively extracted with petroleum ether (10 L \times 2) and H₂O/ethanol (20:80, v/v, 10 L \times 4) at room temperature for 72 h, respectively. The combined 80% ethanol extract was evaporated under reduced pressure to afford a black residue (510.0 g), which was suspended in water and submitted for liquid–liquid partitioning with petroleum ether (1.0 L \times 5), ethyl acetate (1.0 L \times 5) and *n*-BuOH (1.0 L \times 5), successively. The EtOAc extract (120.0 g) was subjected to a MCI gel CHP-20P column, and

Table 2
 ^1H NMR (600 MHz) and ^{13}C NMR (150 MHz) Data of Compounds 5–6 in $\text{DMSO}-d_6$.

position	5		6	
	δ_{C} , type	δ_{H} (J in Hz)	δ_{C} , type	δ_{H} (J in Hz)
1	57.4 CH	1.66 (m)	57.2 CH	1.63 (m)
2	24.6 CH_2	1.61 (m) 1.47 (m)	24.5 CH_2	1.68 (m) 1.40 (m)
3	39.8 CH_2	1.77 (dt, 11.9, 6.3) 1.34 (m)	39.8 CH_2	1.77 (dt, 11.5, 5.4) 1.34 (m)
4	86.6 C		86.6 C	
5	46.0 CH	1.41 (m)	44.7 CH	1.94 (dd, 11.4, 8.4)
6	29.1 CH	0.37 (dd, 10.8, 9.6)	30.5 CH	0.34 (dd, 11.4, 9.6)
7	26.0 CH	0.50 (ddd, 10.8, 9.6, 6.0)	25.8 CH	0.50 (ddd, 11.4, 9.6, 6.0)
8	19.0 CH_2	1.70 (m) 0.84 (m)	19.0 CH_2	1.38 (m) 1.52 (dd, 12.7, 6.0)
9	44.7 CH_2	1.57 (dt, 13.1, 6.8) 1.38 (m)	42.6 CH_2	1.57 (dt, 12.6, 6.0) 1.34 (m)
10	73.0 C		70.3 C	
11	19.3 C		21.1 C	
12	28.7 CH_3	0.98 (s)	28.6 CH_3	0.98 (s)
13	16.9 CH_3	1.03 (s)	16.9 CH_3	1.12 (s)
14	21.9 CH_3	1.21 (s)	21.4 CH_3	1.23 (s)
15	20.5 CH_3	1.00 (s)	30.0 CH_3	1.08 (s)
1'	97.7 CH	4.25 (d, 8.1)	97.6 CH	4.30 (d, 7.8)
2'	73.5 CH	2.87 (td, 8.1, 5.1)	73.9 CH	2.90 (t, 8.4)
3'	77.3 CH	3.10 (td, 8.1, 4.9)	77.0 CH	3.10 (t, 8.4)
4'	70.3 CH	3.01 (m)	70.0 CH	3.00 (m)
5'	76.8 CH	2.99 (m)	76.9 CH	3.00 (m)
6'	61.3 CH_2	3.61 (ddd, 11.5, 5.6, 1.9) 3.39 (dt, 11.5, 5.8)	61.2 CH_2	3.62 (d, 11.4) 3.39 (dd, 12.6, 4.8)

eluted with gradient H_2O -MeOH (1:0 to 0:1, v/v), and finally with acetone, to yield six fractions (Fr. A-F). The 100% MeOH eluted fraction (Fr. A, 5.4 g) was put on a Sephadex LH-20 column and eluted with MeOH to yield 9 subfractions (Fr. A1-9). Fr. A4 (653.2 mg) was separated on a silica gel column (CH_2Cl_2 -MeOH 30:1 to 10:1, v/v) and further purified by ODS column (MeOH- H_2O 90:10) to afford compound 4 (6.2 mg). The 80% MeOH eluted fraction (Fr. B, 10.7 g) was chromatographed over a silica gel column (CH_2Cl_2 -MeOH 40:1 to 0:1, v/v) to yield 6 subfractions (Fr. B1-6). Fr. B3 (301.0 mg) was separated on a silica gel column (CH_2Cl_2 -MeOH 20:1 to 10:1, v/v), followed by a Sephadex LH-20 column (100% MeOH) to afford compound 2 (8.5 mg). Fr. B4 (4.0 g) was chromatographed over a silica gel column (CH_2Cl_2 -MeOH 15:1 to 5:1, v/v) and further purified by ODS column (MeOH- H_2O 80:20) to afford compound 1 (4.2 mg). The 60% MeOH eluted fraction (Fr. C, 19.1 g) was subjected to a silica gel column (CH_2Cl_2 -MeOH 10:1 to 0:1, v/v) to yield 5 subfractions (Fr. C1-5). Fr. C1 (1.2 g) was submitted to a Sephadex LH-20 column using MeOH as eluent, and then purified on a silica gel column (CH_2Cl_2 -MeOH 20:1) to afford compound 6 (6.7 mg). Fr. C3 (1.4 g) was sequentially chromatographed over Sephadex LH-20 column and ODS column (MeOH- H_2O 70:30) to afford compound 3 (46.8 mg). Similarly, fraction D (40% MeOH eluted fraction, 58.6 g) was chromatographed over a silica gel column (CH_2Cl_2 -MeOH 10:1 to 0:1, v/v) and further separated by repeated silica gel column and Sephadex LH-20 column to afford compound 5 (9.0 mg). The *n*-BuOH extract (150.0 g) was also loaded on a MCI gel CHP-20P column (H_2O -MeOH, 1:0 to 0:1, v/v) to yield six fractions (Fr. G-L). Fraction J (40% MeOH eluted fraction from *n*-BuOH extract, 17.8 g) was separated on a silica gel column (CH_2Cl_2 -MeOH 10:1 to 1:1, v/v) to yield 3 subfractions (Fr. J1-3). Fr. J1 (1.5 g) was subject to a Sephadex LH-20 column chromatograph eluting with MeOH and further purified by silica gel column (CH_2Cl_2 -MeOH 10:1 to 5:1, v/v) to afford compound 8 (4.5 mg). Similarly, Fr. J2 (4.7 g) was separated over Sephadex LH-20 column (100% MeOH), silica gel column (CH_2Cl_2 -MeOH 4:1 to 1:1, v/v) and further purified by ODS column (MeOH- H_2O 60:40) to afford compound 7 (124.9 mg).

Compound 1: white amorphous powder; $[\alpha]_D^{20} - 200$ (c 0.12, MeOH);

$\text{Mo}_2(\text{OAc})_4$ induced ECD $\lambda_{\text{max}}(\Delta\epsilon)$ 317 (-0.96); IR (film) ν_{max} 3403, 2945, 2927, 2860, 1661, 1639, 1601, 1455, 1374, 1307, 1262, 1209, 1164, 1135, 1047, 1003, 983, 924, 900, 855, 830, 805 cm^{-1} ; ^1H NMR and ^{13}C NMR data, see Table 1; HRESIMS m/z 499.3384 [M + Na] $^+$ (calcd for $\text{C}_{29}\text{H}_{48}\text{O}_5\text{Na}$, 499.3399).

Compound 2: white amorphous powder; $[\alpha]_D^{20} - 77$ (c 0.26, MeOH); $\text{Mo}_2(\text{OAc})_4$ induced ECD $\lambda_{\text{max}}(\Delta\epsilon)$ 308 (-0.22); IR (film) ν_{max} 3423, 2923, 2854, 1718, 1647, 1457, 1374, 1308, 1260, 1216, 1158, 1122, 1099, 1050, 985, 939, 907, 803 cm^{-1} ; ^1H NMR and ^{13}C NMR data, see Table 1; HRESIMS m/z 427.3183 [M + H - H_2O] $^+$ (calcd for $\text{C}_{28}\text{H}_{43}\text{O}_3$, 427.3212).

Compound 3: white amorphous powder; $[\alpha]_D^{20} - 17$ (c 0.24, MeOH); IR (film) ν_{max} 3386, 2924, 2855, 1739, 1644, 1455, 1375, 1311, 1265, 1220, 1192, 1168, 1073, 1025, 966, 926, 892, 820 cm^{-1} ; ^1H NMR and ^{13}C NMR data, see Table 1; HRESIMS m/z 687.3701 [M + Na] $^+$ (calcd for $\text{C}_{36}\text{H}_{56}\text{O}_{11}\text{Na}$, 687.3720).

Compound 4: white amorphous powder; $[\alpha]_D^{20} - 160$ (c 0.15, MeOH); IR (film) ν_{max} 3398, 3369, 2971, 2926, 2870, 1691, 1551, 1454, 1384, 1312, 1279, 1253, 1234, 1122, 1053, 985, 918, 829, 809 cm^{-1} ; ^1H NMR and ^{13}C NMR data, see Table 1; HRESIMS m/z 617.4107 [M - H] $^-$ (calcd for $\text{C}_{36}\text{H}_{57}\text{O}_8$, 617.4053).

Compound 5: colorless oil; $[\alpha]_D^{20} - 50$ (c 0.24, MeOH); IR (film) ν_{max} 3380, 2923, 2860, 1740, 1640, 1455, 1378, 1300, 1253, 1156, 1077, 1021, 934, 893, 860, 822 cm^{-1} ; ^1H NMR and ^{13}C NMR data, see Table 2; HRESIMS m/z 423.2347 [M + Na] $^+$ (calcd for $\text{C}_{21}\text{H}_{36}\text{O}_7\text{Na}$, 423.2359).

Compound 6: colorless oil; $[\alpha]_D^{20} - 63$ (c 0.19, MeOH); IR (film) ν_{max} 3381, 2957, 2921, 2868, 1718, 1639, 1575, 1539, 1456, 1375, 1329, 1313, 1289, 1256, 1210, 1153, 1076, 1038, 1020, 925, 899, 859, 804 cm^{-1} ; ^1H NMR and ^{13}C NMR data, see Table 2; HRESIMS m/z 423.2351 [M + Na] $^+$ (calcd for $\text{C}_{21}\text{H}_{36}\text{O}_7\text{Na}$, 423.2359).

Compound 7: colorless gum; $[\alpha]_D^{20} - 160$ (c 0.20, MeOH); IR (film) ν_{max} 3325, 2954, 2925, 2858, 1624, 1601, 1510, 1445, 1355, 1267, 1226, 1167, 1075, 1046, 1022, 896, 829 cm^{-1} ; ^1H NMR and ^{13}C NMR data, see Table 3; HRESIMS m/z 681.2356 [M + Na] $^+$ (calcd for $\text{C}_{30}\text{H}_{42}\text{O}_{16}\text{Na}$, 681.2371).

Table 3
 ^1H NMR (600 MHz) and ^{13}C NMR (150 MHz) Data of Compounds **7–8** in DMSO- d_6 .

Position	7		8	
	δ_{C} , type	δ_{H} (J in Hz)	δ_{C} , type	δ_{H} (J in Hz)
1	110.71 C		108.0 C	
2	156.09 C		156.6 C	
3	96.3 CH	6.02 (s)	98.5 CH	6.25 (br s)
4	156.6 C		157.1 C	
5	96.3 CH	6.02 (s)	97.8 CH	6.10 (d, 2.2)
6	156.09 C		152.9 C	
7	30.1 CH	4.68 (t, 8.1)	38.3 CH	3.25 (m)
8	31.3 CH ₂	2.01 (m)	30.1 CH ₂	1.32 (m)
9	28.1 CH ₂	1.16 (m)	26.7 CH ₂	1.24 (m)
10	31.4 CH ₂	1.22 (m)	31.1 CH ₂	1.13 (m)
11	22.1 CH ₂	1.22 (m)	22.0 CH ₂	1.12 (m)
12	14.1 CH ₃	0.81 (t, 7.2)	13.9 CH ₃	1.19 (m)
13	110.65 C		77.5 C	0.80 (t, 7.2)
14	156.06 C		101.7 C	
15	96.3 CH	6.02 (s)	84.3 CH	4.34 (d, 6.0)
16	156.6 C		69.7 CH	3.87 (m)
17	96.3 CH	6.02 (s)	61.7 CH ₂	3.68 (m)
18	156.06 C		175.5 C	3.47 (m)
1'	100.55 CH	4.66 (d, 7.8)	100.9 CH	4.69 (d, 7.8)
2'	73.2 CH	3.13 (m)	73.2 CH	3.16 (m)
3'	77.00 CH	3.19 (m)	77.0 CH	3.25 (m)
4'	69.5 CH	3.17 (m)	69.5 CH	3.18 (m)
5'	76.6 CH	3.22 (m)	76.5 CH	3.25 (m)
6'	60.6 CH ₂	3.66 (m)	60.6 CH ₂	3.68 (m)
1''	100.50 CH	4.65 (d, 7.8)		3.52 (m)
2''	73.2 CH	3.13 (m)		
3''	76.98 CH	3.19 (m)		
4''	69.5 CH	3.17 (m)		
5''	76.6 CH	3.22 (m)		
6''	60.6 CH ₂	3.66 (m)		
OH-2		9.53 (br s)		
OH-6		9.53 (br s)		9.55 (m)
OH-13				6.29 (br s)
OH-14		9.53 (br s)		6.93 (br s)
OH-16				4.96 (d 4.8)
OH-17				4.83 (t 5.4)
OH-18		9.53 (br s)		

Compound 8: colorless gum; $[\alpha]_{\text{D}}^{20}$ -233 (c 0.12, MeOH); ECD λ_{max} ($\Delta\epsilon$) 235 (-21.6), 276 (1.00), 309 (0.40); IR (film) ν_{max} 3331, 2927, 2857, 1780, 1625, 1513, 1439, 1361, 1227, 1191, 1166, 1136, 1074, 1043, 1024, 892, 830 cm^{-1} ; ^1H NMR and ^{13}C NMR data, see [Table 3](#); HRESIMS m/z 569.1825 $[\text{M} + \text{Na}]^+$ (calcd for $\text{C}_{24}\text{H}_{34}\text{O}_{14}\text{Na}$, 569.1846).

2.4. $\text{Mo}_2(\text{AcO})_4$ -induced circular dichroism measurement and ECD calculation

$\text{Mo}_2(\text{AcO})_4$ -induced circular dichroism spectra of compounds **1** and **2** were obtained according to our reported method [15]. After the addition of tested sample to freshly prepared $\text{Mo}_2(\text{AcO})_4$ solution, the CD spectrum was recorded immediately and then scanned every 10 min until a stationary $\text{Mo}_2(\text{AcO})_4$ -induced CD spectrum was observed.

In order to investigate the absolute configuration of compound **8**, quantum chemical ECD calculation were conducted. The stable conformational analysis of compound **8** was performed with CONFLEX software based on MMFF94S molecular force field, with an energy cut off of 3 kcal mol^{-1} . The selected conformers were further optimized with density functional theory (DFT) method at the B3LYP/6-31G (d) level by using Gaussian 09 software. The theoretical ECD of chosen conformers of **8** were calculated using time-dependent density

functional theory (TDDFT) method at B3LYP/6-311++G (2d, p) level in methanol. The final ECD curves were generated with SpecDis1.62 software based on Boltzmann distribution theory, and corrected based on the UV correction. The calculated ECD spectra of four isomers were then compared with the experimental spectrum of **8**.

2.5. Determination of the absolute configuration of monosaccharides

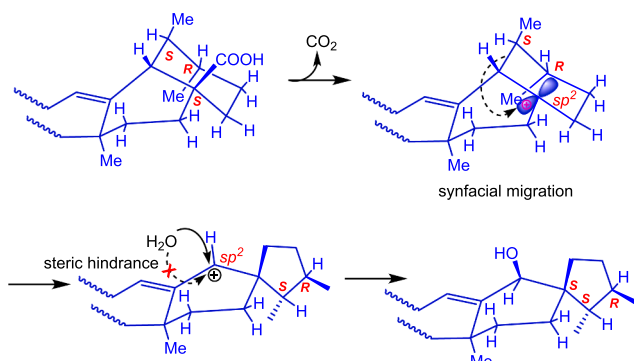
The absolute configuration of monosaccharides in compounds **3–5** and **7** were determination based on GC-MS method with pre-column derivatization. Briefly, compounds (**3–5**, **7**) (each 2.0 mg) were dissolved in MeOH (0.5 mL) and submitted for reaction with 2 M HCl (2 mL) at 100 °C for 4 h, respectively. After hydrolysis, the yield mixture was washed with *n*-hexane for three times (2 mL each). The aqueous layer was collected and evaporated under reduced pressure, followed by reaction with *L*-cysteine methyl ester hydrochloride (2 mg) at 80 °C for 1 h. Then *N*-trimethylsilylimidazole (0.3 mL) was added to the mixture and allowed reaction for another 1 h. After that, 1 M HCl (5 mL) was added and the mixture was extracted with *n*-hexanes for three times (5 mL each). The hexane layer was combined and submitted for GC-MS analysis according to our previously reported method [16]. The absolute configurations were determined by comparing the retention times of their derivatives prepared in a similar way from standard sugars, as *D*-glucose at 11.70 min, and *L*-rhamnose at 9.77 min.

2.6. Antimicrobial assay

Micro broth dilution assay was conducted to evaluate the minimum inhibitory concentrations (MICs) of all isolates against three bacteria (*Staphylococcus aureus* ATCC 25923, *Bacillus subtilis* ATCC 6633, and *Escherichia coli* ATCC 25922) and five fungi (*Candida albicans* ATCC MYA-2876, *Cryptococcus neoformans* ATCC 208821, *Candida parapsilosis* ATCC 22019, *Aspergillus fumigatus* CCTCC AF 93,048 and *Aspergillus niger* CCTCC AF 93021) according to reported method [17]. Tested samples were dissolved in DMSO and then diluted with LB/RPMI-1640 culture medium to prepare a serial samples at seven different concentrations (1.56–100 $\mu\text{g/mL}$). One hundred microliter of microbial suspensions containing 1×10^6 cfu/mL of bacteria or 2×10^3 cfu/mL of fungi, and 1 μL samples were added to each well of 96-well microplates sequentially. After co-incubation (bacteria: at 28 °C for 24 h; fungi: at 28 °C for 48 h except *A. niger* which was incubated at 37 °C), MTT (10 μL , 5 mg/mL) was added to each well and incubated for another four hours. Then the supernatant was removed and 150 μL DMSO was added. The optical density (OD) of each well was measured on a microplate reader (Bio Tek Instruments, Inc) at the wavelength of 490 nm. The MIC was defined as the minimal concentration of the test sample capable of completely inhibiting visual growth of a microorganism. Ciprofloxacin and amphotericin B were used as positive controls against bacteria and fungi, respectively.

3. Results and discussion

Compound **1** was obtained as white amorphous powder. Positive high-resolution electrospray ion mass (HRESIMS) of **1** showed a pseudomolecular ion peak at m/z 499.3384 ($[\text{M} + \text{Na}]^+$, calcd for $\text{C}_{29}\text{H}_{48}\text{O}_5\text{Na}$, 499.3399), allowing the assignment of a molecular formula $\text{C}_{29}\text{H}_{48}\text{O}_5$ for **1** with six degrees of unsaturation. The IR spectrum of **1** showed a broad absorption band for hydroxyl groups at 3403 cm^{-1} . The ^1H NMR spectrum of **1** (in DMSO- d_6 , 600 MHz, [Table 1](#)) displayed four singlet methyl groups (δ_{H} 0.91, 0.99, 1.07, 1.32), two doublet methyl groups [δ_{H} 0.84 (d, 3H, $J = 6.6$ Hz), 0.98 (d, 3H, $J = 7.2$ Hz)], an olefinic proton signal [δ_{H} 5.66 (t, 1H, $J = 3.0$ Hz)], four oxygenated methine proton signals (δ_{H} 3.11, 3.53, 3.93, 4.25), and a hydroxyl methylene group (δ_{H} 3.19, 3.38). The ^{13}C NMR and DEPT spectral data of **1** (in DMSO- d_6 , 150 MHz, [Table 1](#)) indicated 29 carbon resonances for two olefinic carbons (δ_{C} 117.7, 142.1), six sp^3 methyls,



Scheme 1. Plausible biogenetic pathway of 19(18→17)-abeo-28-norursane.

eight sp^3 methylenes (one oxygen-bearing methylene at δ_C 63.7), eight sp^3 methines (four oxygen-bearing methine at δ_C 65.8, 67.5, 70.8, 75.7), and five sp^3 quaternary carbons (Table 1). All of the proton signals were assigned to the corresponding carbons through carefully HSQC spectral analysis. The NMR data of **1** were similar to those of known nor-triterpenoid phlomitetraol B, which possessed a 19(18→17)-abeo-28-norolean-12-ene skeleton [18]. In comparison with phlomitetraol B, obvious difference of NMR data were observed at ring E. The singlet proton signals for two tertiary methyls (Me-29 and Me-30) in phlomitetraol B were replaced by two doublet secondary methyl signals [δ_H 0.84 (d, 3H, $J = 6.6$ Hz), 0.98 (d, 3H, $J = 7.2$ Hz)] in compound **1**. Additionally, a quaternary carbon and a methylene signal disappeared, while two extra methine groups [δ_H 0.85 (1H, m), δ_C 54.0; δ_H 1.78 (1H, m), δ_C 40.5] were present in compound **1**. The above NMR analysis indicated compound **1** contained a norursane rather than noroleanane skeleton. This conclusion was supported by unambiguous HMBC correlation signals from H₃-29 (δ_H 0.98) to C-17 (δ_C 49.6), C-19 (δ_C 54.0) and C-20 (δ_C 40.5), and from H₃-30 (δ_H 0.84) to C-19 (δ_C 54.0), C-20 (δ_C 40.5) and C-21 (δ_C 33.2) (Fig. 2). Besides ring E, the NMR data of compound **1** in rings A-D closely resembled phlomitetraol B, except for one extra hydroxy group signal (δ_H 4.05, d, $J = 3.6$ Hz, OH-6) and obvious downfield shift carbon resonance of C-6 (δ_C 65.8). In combination of HRESIMS data and HMBC signals from OH-6 to C-5 (δ_C 46.4) and C-6, the extra hydroxy group was located at C-6. The location of other hydroxy groups at C-2, C-3, C-18 and C-23 were deduced from HMBC correlation signals as shown in Fig. 2. Thus, the planar structure of compound **1** was determined.

The relative configuration of **1** was determined by extensive analysis of the 1H NMR and NOESY data. In NOESY spectrum, obvious correlation signals (Fig. 3) were observed between H-2 (δ_H 3.53) and H-1 β (δ_H 1.78), H₃-24 (δ_H 0.91) and H₃-25 (δ_H 1.32), between H-3 (δ_H 3.11) and H-1 α (δ_H 0.70) and H-5 (δ_H 1.16), indicating the 2 α , 3 β orientation of OH-2 and OH-3, respectively. This conclusion was also supported by the large coupling constant between H-2 and H-3 ($J_{H-2,3} = 9.5$ Hz) [19]. The orientation of hydroxy group at C-6 was determined as β based on observed NOESY correlation between H-5 (δ_H 1.16) and H-6 (δ_H 4.25). The hydroxy group at C-18 oriented as β position was confirmed by the NOESY correlations between H-18 (δ_H 3.93) and H-16 α (δ_H 1.60) and H₃-27 (δ_H 0.99). The S^* configuration of C-17 was deduced based on the NOESY correlations of H-18 with Me-29 (δ_H 0.98) and biogenetic consideration [20]. The proposed biogenetic pathway of 19(18→17)-abeo-28-norursane from ursane with 28-carboxyl moiety was shown in scheme 1. The in situ Mo₂(OAc)₄ complex-induced CD spectrum of **1** exhibited a negative Cotton effect at 317 nm (Fig. 5), indicating the absolute R configuration for both C-2 and C-3 [21]. In combination with the results of relative configuration analysis, the absolute configuration of C-6, C-17 and C-18 were determined as R , S and S , respectively. Therefore, the structure of compounds **1** was determined as (2*R*,3*R*,6*R*,17*S*,18*S*)-19(18→17)-abeo-28-norurs-12-ene-2,3,6,18,23-pentaol, and named syzygiumursanolide A.

Syzygiumursanolide B (**2**) displayed a pseudomolecular ion peak at m/z 427.3183 ($[M + H-H_2O]^+$, calcd for C₂₈H₄₃O₃, 427.3212) in positive HRESIMS spectrum, predicating a molecular formula of C₂₈H₄₄O₄ for **2**. The IR and NMR data of **2** (Table 1) showed high similarity to those of compound **1**, suggesting compound **2** was also a 28-norursane with spirocyclic skeleton through C-17. Compared to compound **1**, the 1H and ^{13}C NMR spectroscopic data of **2** in rings B-E were almost identical, indicating that both compounds possessed the same plane structure and absolute configuration in these moieties. For ring A fragment, signals associated with oxygenated methylene (CH₂OH) and singlet methyl group (Me-24) in **1** were absent, while the presence of an exomethylene group (δ_H 5.21, 5.35; δ_C 106.4) in **2** were observed. HMBC correlations from H₂-23 (δ_H 5.21, 5.35) to C-3 (δ_C 77.8), C-4 (δ_C 149.2) and C-5 (δ_C 51.0), from H-3 (δ_H 3.50) and H-5 (δ_H 1.60) to C-4 enabled the location of exomethylene at C-4 (Fig. 2). As described for compound **1**, the orientation of three hydroxy groups at C-2, C-3, and C-18 were also determined as 2 α , 3 β , 18 β , respectively. Although the chemical shift values for H-6 and OH-6 were overlapped (δ_H 4.20), the peak shape of H-6 (brs) and the significant downfield shift of chemical resonance of H₃-25 (δ_H 1.00, +0.32) and H₃-26 (δ_H 1.13, +0.34) due to 1,3-diaxial interactions [22], revealed the β orientation of hydroxy group at C-6. Similar to compound **1**, the absolute configuration of 2*R*,3*R*,6*R*,17*S*,18*S* were determined based on displayed negative peak at 308 nm in induced CD spectrum after mixed with Mo₂(OAc)₄ in DMSO (Fig. 5). Therefore, the structure of syzygiumursanolide B (**2**), as shown in Fig. 1, was determined to be (2*R*,3*R*,6*R*,17*S*,18*S*)-19(18→17)-abeo-24,28-norurs-4(23),12-diene-2,3,6,18-tetraol.

A molecular formula of C₃₆H₅₆O₁₁ was determined for compound **3** based on HRESIMS (m/z 687.3701, $[M + Na]^+$, calcd for C₃₆H₅₆O₁₁Na, 687.3720) as well as ^{13}C NMR data. The IR spectrum of **3** showed a broad absorption band for hydroxyl groups at 3386 cm⁻¹, as well as absorption of carbonyl group at 1739 cm⁻¹. The 1H NMR spectrum of **3** (in DMSO-*d*₆, 600 MHz, Table 1) displayed four singlet methyl groups (δ_H 0.90, 0.96, 1.05 and 1.28), one doublet methyl group [δ_H 0.95 (d, 3H, $J = 6.6$ Hz)], an olefinic proton at δ_H 5.21, a pair of terminal olefinic protons [δ_H 4.67 (1H, brs), 4.58 (1H, brs)], and an anomeric proton signal at δ_H 5.18 (d, 1H, $J = 8.2$ Hz). The ^{13}C NMR and DEPT spectral data of **3** (in DMSO-*d*₆, 150 MHz, Table 1) exhibited 36 carbon signals, including one carbonyl carbon (δ_C 174.4), four olefinic carbons (δ_C 104.8, 125.6, 136.7, 152.8), five sp^3 methylenes (one oxygenated methylene at δ_C 63.7), seven sp^3 methines (three oxygenated methine at δ_C 65.8, 67.5, 75.7), six sp^3 quaternary carbons, and a group of carbon signals for a hexose (δ_C 94.3, 77.6, 76.6, 72.3, 69.6, 60.7). Acid hydrolysis and further GC-MS analysis of the trimethylsilyl ether derivative of sugar moiety revealed the presence of *D*-glucose. The NMR spectroscopic data of **3** were very similar to those of known compound 2*\alpha*,3*\beta*,23-trihydroxyurs-12,20(30)-dien-28-oic acid β -*D*-glucopyranoside [23], except for the replacement of a methylene group with an oxygenated methine group (δ_H 4.24; δ_C 65.8), along with the appearance of an extra hydroxy group (δ_H 4.05, d, $J = 4.2$ Hz) in **3**, suggesting that compound **3** was a hydroxyl derivative of 2*\alpha*,3*\beta*,23-trihydroxyurs-12,20(30)-dien-28-oic acid β -*D*-glucopyranoside. The location of hydroxy group at C-6 was deduced by the downfield shift of carbon resonance for C-6 (δ_C 65.8 in **3** vs δ_C 17.7 in known compound) [23], and supported by unambiguous correlation signals from OH-6 (δ_H 4.05) to C-5 (δ_C 46.5) and C-6 in the HMBC spectrum. The HMBC correlation from H-1' (δ_H 5.18) to C-28 (δ_C 174.4) confirmed the linkage of sugar moiety to C-28. The β -configuration of the glucose was determined based on the coupling constant of anomeric proton ($J = 8.2$ Hz) [24]. The 2 α , 3 β , 6 β orientation of three hydroxyl groups were determined to be the same as those in compound **1** based on NOESY experiment and coupling constant analysis as described above. Based on above evidence, the structure of **3** was elucidated as 2*\alpha*,3*\beta*,6 β ,23-tetrahydroxyurs-12,20(30)-dien-28-oic acid β -*D*-glucopyranoside, and named syzygiumursanolide C.

The molecular formula of syzygiumursanolide D (**4**) was determined

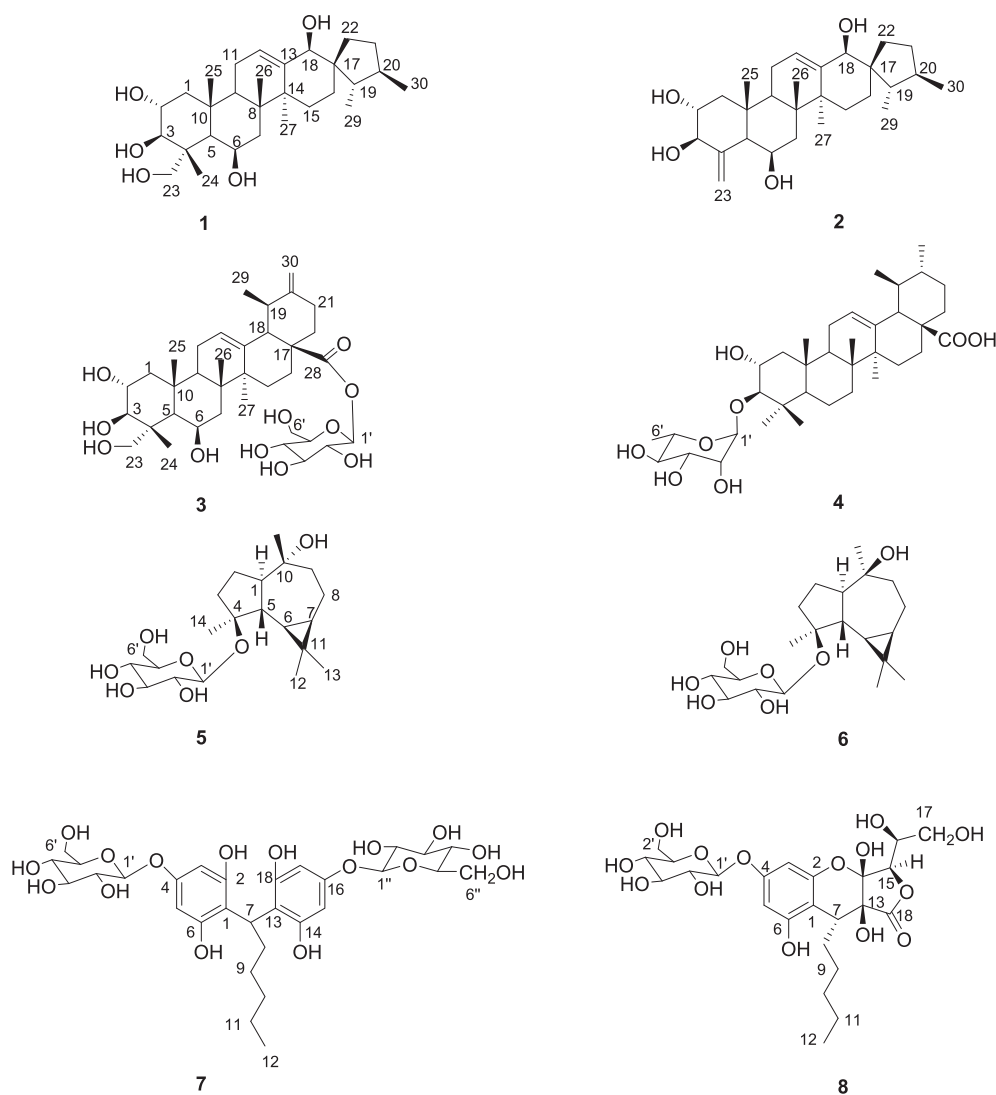


Fig. 1. Chemical structures of compounds 1–8.

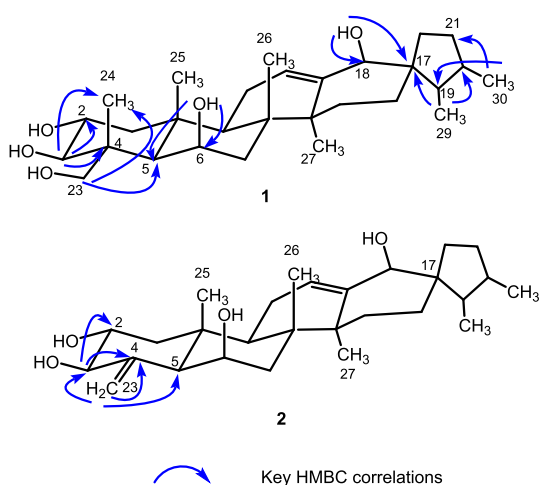


Fig. 2. Key HMBC correlations of compounds 1 and 2.

as $C_{36}H_{58}O_8$ based on observed pseudomolecular ion peak at m/z 617.4107 ($[M-H]^-$, calcd for $C_{36}H_{57}O_8$, 617.4053). The 1H and ^{13}C NMR data of **4** (in $DMSO-d_6$, Table 1) suggested it was an ursane-type triterpenoid. Beside 30 carbon resonances attributed to triterpenoid

aglycone, ^{13}C NMR and DEPT spectra also exhibited a group of rhamnose carbons (δ_C 103.3, 71.8, 70.8, 70.5, 69.4, 17.8) [25]. The spectroscopic data of **4** were closely related to those of known compound grandoside [26], except for the absence of a methylene signal (δ_H 1.84, 2.15; δ_C 26.3 in grandoside) for C-2 along with the appearance of an extra oxygenated methine carbon (δ_H 3.54; δ_C 66.4), indicating that compound **4** was the 2-hydroxyl derivative of grandoside. This conclusion was confirmed by the HMBC correlations of OH-2 (δ_H 4.18) with C-1 (δ_C 46.7), C-2 (δ_C 66.4) and C-3 (δ_C 94.6). The attachment of rhamnose to aglycone at C-3 was established by the HMBC correlations from H-3 (δ_H 2.84) to C-1' (δ_C 103.3), and from anomeric proton (δ_H 4.63, H-1') of sugar to C-3. The sugar moiety of **4** were determined to be α -L-rhamnose based on the peak shape of anomeric proton (br s) [24], and acid hydrolysis and GC-MS analysis result as described for **3**. Similar to compounds **1**–**3**, the orientation of two hydroxy groups at C-2 and C-3 in compound **4** were determined as 2α , 3β based on the large value of $J_{H-2,3}$ (9.0 Hz), as well as the NOESY correlation signals between H-2 (δ_H 3.53) and H-1 β (δ_H 1.86)/H₃-25 (δ_H 0.92), and between H-3 (δ_H 2.84)/H-1 α (δ_H 0.82)/H-5 (δ_H 0.80)/H₃-23 (δ_H 0.92). Therefore, the structure of syzygiumursanolide D was elucidated as $2\alpha,3\beta$ -hydroxyurs-12-en-28-oic acid 3α -L-rhamnopyranoside.

Compound **5** was obtained as colorless oil. Its molecular formula was established as $C_{21}H_{36}O_7$ based on HRESIMS data (m/z 423.2347, $[M + Na]^+$; calcd for $C_{21}H_{36}O_7Na$, 423.2359) and ^{13}C NMR spectral

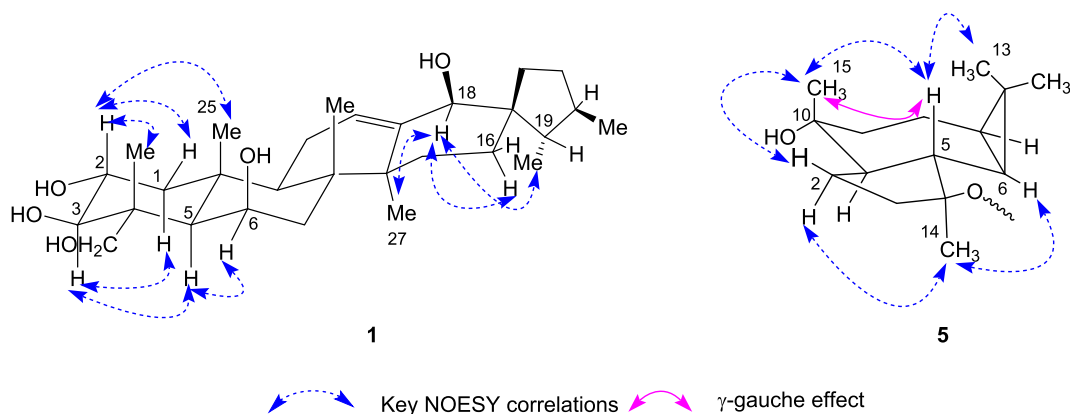


Fig. 3. Key NOESY correlations of compounds 1 and 5, and the steric effects in 5.

analysis. The IR spectrum of **5** showed a broad absorption band for hydroxy groups at 3380 cm^{-1} . The ^1H NMR spectrum of **5** (in $\text{DMSO-}d_6$, 600 MHz, Table 2) displayed characteristic proton signals for aromadendrane-type sesquiterpenoid, including four tertiary methyls (δ_{H} 0.98, 1.03, 1.03, 1.21), and two typical cyclopropyl protons [δ_{H} 0.37 (dd, 1H, $J = 10.8, 9.6$ Hz), 0.50 (ddd, 1H, $J = 10.8, 9.6, 6.0$ Hz)]. Besides signals for the core structure, ^1H and ^{13}C NMR spectra also exhibited a group of signals for a hexose (δ_{H} 4.25, d, $J = 8.1$ Hz, H-1'; δ_{C} 97.7, 77.3, 76.8, 73.5, 70.3, 61.3). The presence of β -D-glucose in **5** was determined based on coupling constant analysis of anomeric proton, and GC-MS analysis of yielded monosaccharide trimethylsilyl ether derivative after acid hydrolysis. In HMBC spectrum, cross peak between H-1' and C-4 (δ_{C} 86.6) indicated that the glucose was attached to aglycone by a glycosidic linkage at C-4. Thus, the planar structure of **5** was determined. Since the chemical shifts of two cyclopropyl protons were at relative downfield (δ_{H} 0.37, H-6; δ_{H} 0.50, H-7), 1,5-*trans* aromadendrane skeleton of **5** was deduced (H-1 α , H-5 β) [27]. This conclusion was supported by no NOESY correlation between H-1 (δ_{H} 1.66) and H-5 (δ_{H} 1.41). In the NOESY spectrum, the correlations between H₃-15 (δ_{H} 1.00)/H-5/H-2 β (δ_{H} 1.61), and between H₃-14 (δ_{H} 1.21)/H-6/H-2 α (δ_{H} 1.47), suggested that Me-15 and H-5 were on the same side (β), while Me-14 and H-6 orientated on the other side (α) (Fig. 3). Therefore, the structure of **5** was determined to be 4 β ,10 α -aromadendranediol-4- β -D-glucopyranoside.

Compound **6** was assigned the same molecular formula ($\text{C}_{21}\text{H}_{36}\text{O}_7$) as **5** based on HRESIMS (m/z 423.2351, $[\text{M} + \text{Na}]^+$, calcd for $\text{C}_{21}\text{H}_{36}\text{O}_7\text{Na}$, 423.2359) and ^{13}C NMR data analysis. 2D-NMR analysis further revealed that compounds **5** and **6** possessed identical planar structure. Compared to **5**, the major difference between **5** and **6** was the significant downfield shift of carbon resonance for Me-15 (δ_{C} 20.5 in **5** vs δ_{C} 30.0 in **6**), indicating the conformation of the Me-15 was changed from pseudo-axial in **5** to equatorial in **6**, which released γ -gauche effect from H-5 (Fig. 3). This conclusion was confirmed by the correlation signal of H-1 (δ_{H} 1.63) with H₃-15 (δ_{H} 1.08), while no correlation between H-5 (δ_{H} 1.94) and H₃-15 in the NOESY experiment. Thus, compound **6** was 10-epimer of **5**. Due to the limited quantity, acid hydrolysis was not performed for compound **6**. The presence of β -D-glucopyranose was determined by comparison of NMR data with **5** and biogenetic consideration. Hence, the structure of **6** was determined as 4 β ,10 β -aromadendranediol-4- β -D-glucopyranoside as depicted in Fig. 1.

Compound **7** was obtained as colorless gum. A molecular formula of $\text{C}_{30}\text{H}_{42}\text{O}_{16}$ was assigned for **7** based on HRESIMS (m/z 681.2356, $[\text{M} + \text{Na}]^+$; calcd for $\text{C}_{30}\text{H}_{42}\text{O}_{16}\text{Na}$, 681.2371) and ^{13}C NMR data analysis. The IR spectrum of **7** showed a broad absorption band for hydroxy groups at 3325 cm^{-1} , as well as absorption of benzene moiety ($1624, 1601, 1510$ and 1445 cm^{-1}). The ^1H NMR spectra of **7** (in $\text{DMSO-}d_6$, 600 MHz, Table 3) displayed typical signals for dimeric phloroglucinol glycosides, including four singlet aromatic protons (δ_{H}

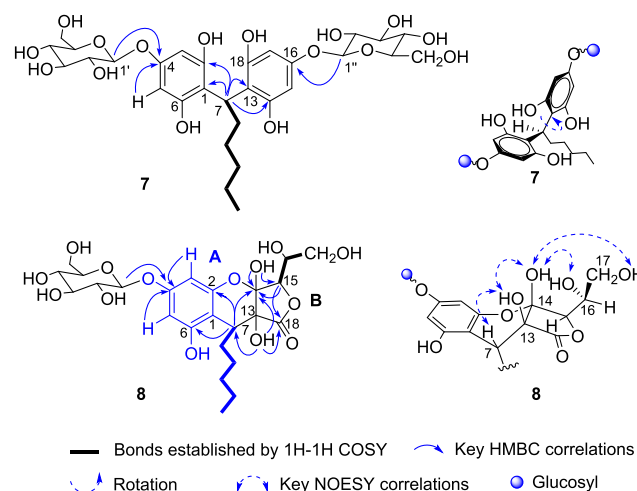


Fig. 4. Key COSY, HMBC and NOESY correlations of compounds 7 and 8, and conformation illustration of compound 7.

6.02, s, 4H), four phenolic hydroxyls (δ_{H} 9.53, brs, 4H), one methine proton at relative low field (δ_{H} 4.68, t, 1H, $J = 8.1$ Hz), and two anomeric protons of glycosyl group (δ_{H} 4.66, d, 1H, $J = 7.8$ Hz, H-1'; δ_{H} 4.65, d, 1H, $J = 7.8$ Hz, H-1''). This conclusion was supported by ^{13}C NMR data (in $\text{DMSO-}d_6$, 150 MHz, Table 3), which exhibited two sets of 1,3,5,6-substituted benzene rings (δ_{C} $156.6 \times 2, 156.09 \times 2, 156.06 \times 2, 110.71, 110.65,$ and 96.3×4), one methine carbon signal at δ_{C} 30.1, and signals for two hexanose (δ_{C} 100.55, 100.50, 77.00, 76.98, $76.6 \times 2, 73.2 \times 2, 69.5 \times 2, 60.6 \times 2$). Besides the signals for dimeric phloroglucinol skeleton, the ^{13}C NMR and DEPT spectral data also revealed the presence of one methyl (δ_{C} 14.1) and four methylenes (δ_{C} 31.4, 31.3, 28.1, 22.1). All of the proton signals were assigned to the corresponding carbons through carefully HSQC spectral analysis. $^1\text{H-}^1\text{H}$ COSY analysis enabled the establishment of a pentyl side chain (Fig. 4). HMBC correlation signals from H-7 (δ_{H} 4.68, t, 1H, $J = 8.1$ Hz) to C-2/C-6 (δ_{C} 156.09), C-1 (δ_{C} 110.71), C-13 (δ_{C} 110.65) and C-14/C-18 (δ_{C} 156.06), as well as the unambiguous COSY signals between H-7 and H₂-8 (δ_{H} 2.01, m, 2H), indicated the pentyl side chain was linked to the dimeric phloroglucinol skeleton via C-7. The HMBC correlations from H-1', H-3/H-5 (δ_{H} 6.02) to C-4 (δ_{C} 156.6), from H-1'', H-15/H-17 (δ_{H} 6.02) to C-16 (δ_{C} 156.6) revealed the linkage of two hexoses to the phloroglucinol core at C-4 and C-16, respectively (Fig. 4). This conclusion was also confirmed by observed identical chemical shifts of H-3, H-5, H-15 and H-17 (δ_{H} 6.02, s, 4H). Both hexoses were identified as β -D-glucopyranose based on coupling constant of their anomeric protons ($J = 7.8$ Hz), and acid hydrolysis and GC-MS analysis result as described for compounds 3–5. It has to be noted that although two

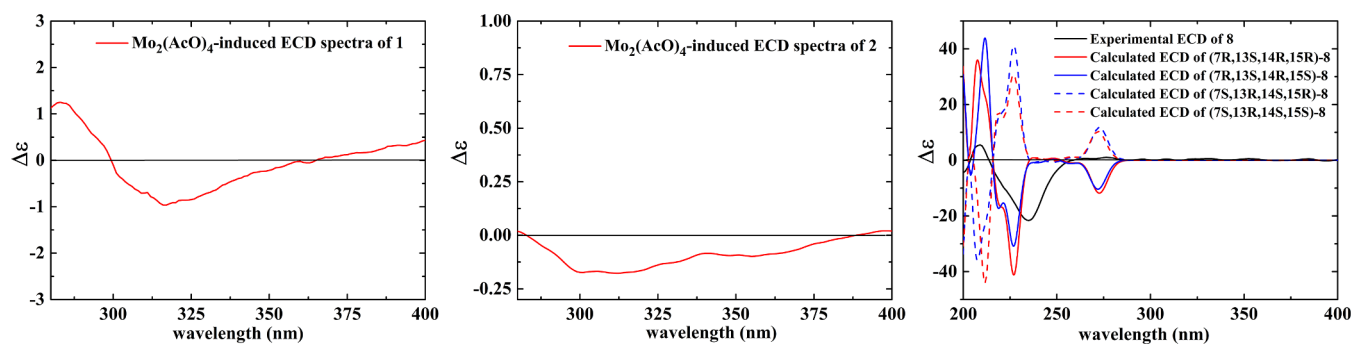


Fig. 5. $\text{Mo}_2(\text{AcO})_4$ -induced circular dichroism spectra of compounds **1** and **2**, and the experimental and calculated ECD spectra of **8**.

substituents at C-7 were same, there was small but obvious difference of carbon resonances between two phloroglucinol moieties of **7** (Table 3), indicating the hindered free rotation of C7-C13 bond due to the big substituents at C-7 (Fig. 4). This conclusion was also supported by the large optical rotation value ($[\alpha]_D^{20} -160$ in MeOH) of **7**. Thus, the structure of compound **7**, named syzygiumone A, was identified as 1,1'-hexylidenebis(2,4,6-trihydroxy-4- β -D-glucopyranosyl)benzene.

The molecular formula of syzygiumone B was deduced as $\text{C}_{24}\text{H}_{34}\text{O}_{14}$ based on observed pseudomolecular ion peak at m/z 569.1825 ($[\text{M} + \text{Na}]^+$, calcd for $\text{C}_{24}\text{H}_{34}\text{O}_{14}\text{Na}$, 569.1846), with 8 degrees of unsaturation. The IR spectrum showed absorption peaks for hydroxyl (3331 cm^{-1}), five membered lacton (1780 cm^{-1}) [28] and benzene ring ($1625, 1513, 1439\text{ cm}^{-1}$). Similar to compound **7**, the ^1H and ^{13}C NMR data (in $\text{DMSO}-d_6$, Table 3) of syzygiumone B also showed characteristic signals for phloroglucinol unit [δ_{H} 9.55 (1H, brs, OH-6), 6.25 (1H, brs, H-3), 6.10 (1H, d, $J = 2.2\text{ Hz}$, H-5); δ_{C} 97.8 (C-5), 98.5 (C-3), 156.6 (C-2), 108.0 (C-1) and 157.1 (C-4)], β -glucopyranose moiety [δ_{H} 4.69, d, 1H, $J = 7.8\text{ Hz}$, H-1'; δ_{C} 100.9, 77.0, 76.5, 73.2, 69.5, 60.6], and pentyl side chain (δ_{C} 31.1, 30.1, 26.7, 22.0, 13.9), indicating syzygiumone B was also a phloroglucinol glucoside with 1-hexyl(2,4,6-trihydroxy-4-glucopyranosyl)benzene unit (fragment A). Compared with **7**, the NMR signals for another phloroglucinol unit was absent in **8**. Instead, a group of signals including one carbonyl (δ_{C} 175.5, C-18), one hemiketal carbon (δ_{C} 101.7, C-14), one oxygenated quaternary carbon (δ_{C} 77.5, C-13), two oxygenated methines (δ_{C} 84.3, C-15; δ_{C} 69.7, C-16), and one oxygenated methylene (δ_{C} 61.7, C-17) were observed in ^{13}C and DEPT spectra. Additionally, the carbon resonance for C-7 was obviously downfield shift (from δ_{C} 30.1 in **7** to δ_{C} 38.3 in **8**). All of the proton signals were assigned to the corresponding carbons through carefully HSQC and HMBC spectral analysis. $^1\text{H}-^1\text{H}$ COSY spectrum analysis (Fig. 4) revealed the presence of $\text{CHCH}(\text{OH})\text{CH}_2\text{OH}$ moiety. In the HMBC spectrum, the correlation signals (Fig. 4) from OH-13 (δ_{H} 6.29, br s) to C-13, C-14, C-18, from OH-14 (δ_{H} 6.93, br s) to C-13, C-14, and C-15, from H-15 (δ_{H} 4.34, d, $J = 6.0\text{ Hz}$) to C-14 and C-

Table 4

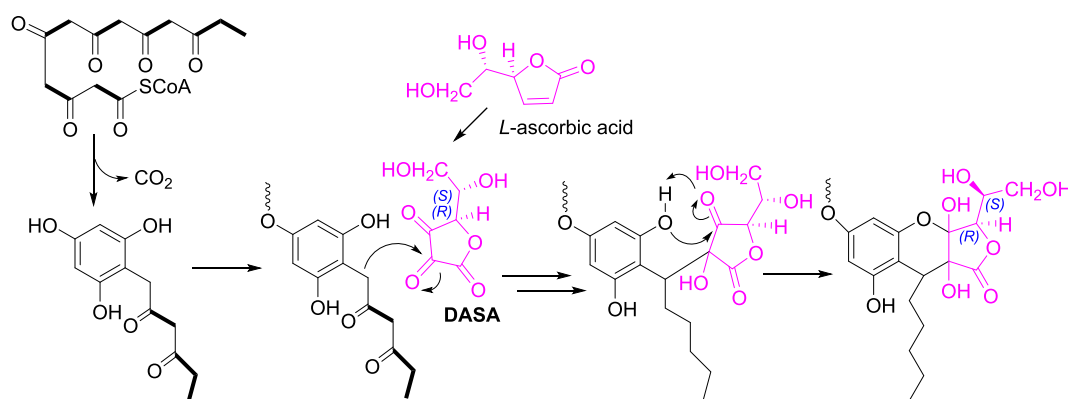
Antimicrobial Activities of isolated triterpenoids from *S. szemaense* (MIC $\mu\text{g}/\text{mL}$).

MIC	1	2	3	4	control
<i>S. aureus</i>	50	25	> 100	50	0.5 ^a
<i>B. subtilis</i>	50	25	> 100	50	0.25 ^a
<i>E. coli</i>	50	25	> 100	50	0.25 ^a
<i>C. albicans</i>	100	> 100	> 100	12.5	2.0 ^b
<i>C. neoformans</i>	50	> 100	> 100	6.25	2.0 ^b
<i>C. parapsilosis</i>	> 100	> 100	> 100	12.5	2.0 ^b
<i>A. fumigatus</i>	100	> 100	> 100	12.5	2.0 ^b
<i>A. niger</i>	> 100	> 100	> 100	25	2.0 ^b

^a Ciprofloxacin. ^bAmphotericin B.

18 enabled the establishment of γ -lacton unit. Thus, the partial structure for fragment B was established as an ascorbyl moiety. The connection of fragment A to B via C7-C13 bond and ether linkage between C-2 and C-14 were deduced based on HMBC correlations from H-7 (δ_{H} 3.25, m) to C-13 and C-14, as well as HRESIMS data. Thus, the gross structure of syzygiumone B was determined.

In the NOESY spectrum, the NOESY correlations between OH-14 and OH-13/OH-16 (δ_{H} 4.96)/OH-17 (δ_{H} 4.83) indicated that OH-13, OH-14, and $-\text{CHOHCH}_2\text{OH}$ group at C-15 were orientated at the same side (assigned as β). In addition, the NOESY correlation between H-7 and OH-13 revealed β -orientation of H-7 (Fig. 4). The absolutely configuration of C-7, C-13, C-14 and C-15 were determined as 7R, 13R, 14R, 15R based on experimental and calculated ECD spectra (Fig. 5). The configuration of C-16 could not be directly determined by NOESY experiment. It has been reported that some phenolics present in plant, including phloroglucinols and catechins could react with *L*-ascorbic acid via its oxidized form dehydroascorbic acid (DASA) to produce ascorbylated derivatives, such as ascorbyl phloroglucinol [29], 8-C-ascorbyl-(-)-epigallocatechin, and 6-C-ascorbyl-(-)-epigallocatechin [30,31]. By comparing the NMR data of ascorbyl unit in syzygiumone B with



Scheme 2. Plausible biogenetic pathway of syzygiumone B (**8**).

reported analogues [29], and in consideration of its phloroglucinol origin, we hypothesized that syzygiumone B was also an adduct of 2-hexyl-5- β -D-glucopyranosylbenzene-1,3,5-triol and DASA (Scheme 2). Since naturally occurring DASA possesses *R,S* configuration for the two chiral carbons (C-15 and C-16 in syzygiumone B, respectively) [28,31], the absolute configuration of C-16 was then concluded as *S**. Due to the limited quantity, acid hydrolysis was not performed for compound 8. The configuration of *D*-glucose was determined based on biogenetic consideration. Based on aforementioned evidence, the structure of syzygiumone B was determined as depicted in Fig. 1.

All the isolates were submitted for antimicrobial assay. Our results (Table 4) revealed that both 28-norursane type triterpenoids, syzygiumursanolides A and B, displayed moderate antibacterial activity against *S. aureus*, *B. subtilis*, and *E. coli* with MIC values at 50 and 25 μ g/mL, respectively. Syzygiumursanolide A also showed weak antifungal activity against *C. albicans* and *C. neoformans*. Among all isolates, syzygiumursanolide D displayed significant antifungal activities against *C. albicans*, *C. neoformans*, *C. parapsilosis*, *A. fumigatus* and *A. niger* with MIC values ranging from 6.25 to 25 μ g/mL. Neither sesquiterpenoids (5 and 6) nor phloroglucinol glucosides (7 and 8) showed any antimicrobial activity at 100 μ g/mL in the current assay.

Ursane-type triterpenoids from natural source have been reported possessing broad-spectrum antimicrobial activities against human and plant pathogens [32,33]. The underlying mechanism of antimicrobial effects of ursane-type triterpenoids was related to disruption of cell membrane integrity of pathogens, as well as regulating genes expression related to peptidoglycan and respiratory metabolisms [34,35]. Structure-activity relationship study suggested that the hydroxyl group in ring A, carboxylic group at C-28 and $\Delta^{12,13}$ double bond were tightly correlated to antimicrobial activities and bioavailability of ursane-type triterpenoids [36,37]. Previously study revealed that the antifungal activities of asiatic acid derived saponins were significantly impacted by saccharide attached position, and monodesmoside with saccharide only attached on C-3 position (3-*O*- α -L-arabinopyranosyl asiatic acid, IC₅₀ = 5 μ g/mL against *Magnaporthe oryzae*) exhibited stronger antifungal activity when compared to bisdesmoside with two sugar chains at both C-3 and C-28 (ilekudinoside D, IC₅₀ > 256 μ g/mL against *M. oryzae*) [33]. In consistent with previous study result, syzygiumursanolide D containing α -L-rhamnose at C-3 position displayed significant antifungal activities, while syzygiumursanolide C containing a glycone moiety at C-28 position showed no inhibitory effects against five pathogenic fungi in the current study. Thus, esterification of C-28 carboxyl group with β -D-glucose might contribute to the losing of antimicrobial activity of syzygiumursanolide C. It is noteworthy that both syzygiumursanolides A and B without C₂₈ carboxyl acid group also displayed moderated antibacterial activity in the current assay. Since polyhydroxyl groups were also considered playing critical roles in antibacterial activity of these triterpenoids [35], we hypothesized that the antibacterial activity of syzygiumursanolides A and B might be due to the syngenetic effects of hydroxyl groups in ring A and $\Delta^{12,13}$ double bond, as well as the spirocyclic moiety. It is well known that bioavailability of ursolic acid *in vivo* is pretty poor [38]. To date, although a lot of work has been done on structural modification and structure-activity relationship study of ursane-type triterpenoids, the impact of spirocyclic moiety on bioactivity and bioavailability of norursane-type triterpenoids are not clear yet. Semi-synthesizing more derivatives of syzygiumursanolides A and B from ursolic acid would help to better understand the contribution of spirocyclic moiety and other substituents in displayed bioactivity of this type of triterpenoids, and promote finding novel therapeutical agents with enhanced bioactivity and bioavailability. Phloroglucinol derivatives are a large class of naturally occurring chemicals with variety of bioactivities, and widely used in pharmaceutical industries [39]. Phloroglucinol itself have been used as anti-spasmodic drug in clinical. Dimeric acylphloroglucinols with methylene linkage from *Hypericum austrobrasilense* and *H. polyanthemum* have been found possessing antinociceptive and

antidepressant activities in mice [40,41]. Although syzygiumones A and B did not show antimicrobial activity in the current study, further bioassay work with different strategies, such as conducting antinociceptive and antidepressant assay, might help to find more biological potential of these phloroglucinol glucosides.

4. Conclusion

In summary, six new terpenoids and two new phloroglucinol derivatives were purified and identified from the leaves of *S. szemaense*. Both syzygiumursanolides A and B share the unusual 28-norursane spirocyclic skeleton. To the best of our knowledge, this is the first report of 19(18 \rightarrow 17)-*abeo*-28-norursane type triterpenoids. Additionally, syzygiumone B contained a unique tricyclic ascorbylated phloroglucinol skeleton featuring with a five-carbon side chain. Both 28-norursanes (Syzygiumursanolides A and B) and one ursane rhamnoside (Syzygiumursanolide D) displayed antibacterial and antifungal activities. The current work would help to enrich phytochemical knowledge of *S. szemaense*, and highlighted syzygium genus as good resources for bioactive natural products discovery.

Declaration of Competing Interest

The authors declare that they have no known competing financial interests or personal relationships that could have appeared to influence the work reported in this paper.

Acknowledgements

This work was supported by the National Natural Science Foundation of China [No. 31401473], and the Fundamental Research Funds for the Central Universities [No. N2020005].

Appendix A. Supplementary data

Supplementary data to this article can be found online at <https://doi.org/10.1016/j.bioorg.2020.104242>.

References

- [1] Y.L. Ren, G.D. Anaya-Eugenio, A.A. Czarnecki, T.N. Ninh, C.H. Yuan, H.B. Chai, D.D. Soejarto, J.E. Burdette, E.J.C. de Blanco, A.D. Kinghorn, Cytotoxic and NF-kappa B and mitochondrial transmembrane potential inhibitory pentacyclic triterpenoids from *Syzygium corticosum* and their semi-synthetic derivatives, *Bioorg. Med. Chem.* 26 (15) (2018) 4452–4460, <https://doi.org/10.1016/j.bmc.2018.07.025>.
- [2] L.K. Chua, C.L. Lim, A.P.K. Ling, S.M. Chye, R.Y. Koh, Anticancer potential of *Syzygium* species: A review, *Plant Food Hum. Nutr.* 74 (1) (2019) 18–27, <https://doi.org/10.1007/s11130-018-0704-z>.
- [3] A. Maroyi, *Syzygium cordatum* Hochst. ex Krauss, An overview of its ethnobotany, phytochemistry and pharmacological properties, *Molecules* 23 (5) (2018), <https://doi.org/10.3390/molecules23051084>.
- [4] G.E.S. Batiha, L.M. Alkzami, L.G. Wasef, A.M. Beshbishy, E.H. Nadwa, E.K. Rashwan, *Syzygium aromaticum* L. (Myrtaceae): traditional uses, bioactive chemical constituents, pharmacological and toxicological activities, *Biomolecules* 10 (2) (2020) 202, <https://doi.org/10.3390/biom10020202>.
- [5] S. Srivastava, D. Chandra, Pharmacological potentials of *Syzygium cumini*: a review, *J. Sci. Food Agric.* 93 (9) (2013) 2084–2093, <https://doi.org/10.1002/jsfa.6111>.
- [6] D.D. Farias, I.A. Neri-Numa, F.F. de Araujo, G.M. Pastore, A critical review of some fruit trees from the Myrtaceae family as promising sources for food applications with functional claims, *Food Chem.* 306 (2020) 125630, <https://doi.org/10.1016/j.foodchem.2019.125630>.
- [7] N. Chhikara, R. Kaur, S. Jaglan, P. Sharma, Y. Gat, A. Panghal, Bioactive compounds and pharmacological and food applications of *Syzygium cumini* - a review, *Food Funct.* 9 (12) (2018) 6097–6116, <https://doi.org/10.1039/c8fo00654g>.
- [8] J.D. Djoukeng, E. Abou-Mansour, R. Tabacchi, A.L. Tapondjou, H. Bouda, D. Lontsi, Antibacterial triterpenes from *Syzygium guineense* (Myrtaceae), *J. Ethnopharmacol.* 101 (1–3) (2005) 283–286, <https://doi.org/10.1016/j.jep.2005.05.008>.
- [9] G.Q. Li, Y.B. Zhang, P. Wu, N.H. Chen, Z.N. Wu, L. Yang, R.X. Qiu, G.C. Wang, Y.L. Li, New phloroglucinol derivatives from the fruit tree *Syzygium jambos* and their cytotoxic and antioxidant activities, *J. Agric. Food Chem.* 63 (47) (2015) 10257–10262, <https://doi.org/10.1021/acs.jafc.5b04293>.
- [10] J. Yang, J.C. Su, X.P. Lei, X.J. Huang, D.M. Zhang, W.C. Ye, Y. Wang,

- Acylphloroglucinol derivatives from the leaves of *Syzygium samarangense* and their cytotoxic activities, *Fitoterapia* 129 (2018) 1–6, <https://doi.org/10.1016/j.fitote.2018.06.002>.
- [11] S.H. Xu, W. Xu, L. Wang, Y.K. Hu, J.P. Liu, Y. Zhao, M.J. Li, F. Li, S.X. Huang, Y. Zhao, New phloroglucinol derivatives with protein tyrosine phosphatase 1B (PTP1B) inhibitory activities from *Syzygium austroyunnanense*, *Fitoterapia* 131 (2018) 141–145, <https://doi.org/10.1016/j.fitote.2018.10.010>.
- [12] F.F. Liu, C.B. Liu, W. Liu, Z.J. Ding, H. Ma, N.P. Seeram, L. Xu, Y. Mu, X.S. Huang, L.Y. Li, New sesquiterpenoids from *Eugenia jambolana* seeds and their anti-microbial activities, *J. Agric. Food Chem.* 65 (47) (2017) 10214–10222, <https://doi.org/10.1021/acs.jafc.7b04066>.
- [13] Y.Y. Li, J.L. Xu, C.H. Yuan, H. Ma, T.T. Liu, F.F. Liu, N.P. Seeram, Y. Mu, X.S. Huang, L.Y. Li, Chemical composition and anti-hyperglycaemic effects of triterpenoid enriched *Eugenia jambolana* Lam. berry extract, *J. Funct. Food* 28 (2017) 1–10, <https://doi.org/10.1016/j.jff.2016.10.021>.
- [14] F.F. Liu, T. Yuan, W. Liu, H. Ma, N.P. Seeram, Y.Y. Li, L. Xu, Y. Mu, X.S. Huang, L.Y. Li, Phloroglucinol derivatives with protein tyrosine phosphatase 1b inhibitory activities from *Eugenia jambolana* seeds, *J. Nat. Prod.* 80 (2) (2017) 544–550, <https://doi.org/10.1021/acs.jnatprod.6b01073>.
- [15] H. Lei, X.P. Lin, L. Han, J. Ma, K.L. Dong, X.B. Wang, J.L. Zhong, Y. Mu, Y.H. Liu, X.S. Huang, Polyketide derivatives from a marine-sponge-associated fungus *Pestalotiopsis heterocornis*, *Phytochemistry* 142 (2017) 51–59, <https://doi.org/10.1016/j.phytochem.2017.06.009>.
- [16] W. Xu, L. Zhang, R. Omar, W. Liu, Z.X. Wei, Z.G. Zhang, Y. Mu, N.P. Seeram, X.S. Huang, H. Ma, L.Y. Li, Barringtogenol C-type triterpenoid saponins from the stem bark of norway maple (*Acer platanoides*), *Planta Med.* 86 (1) (2020) 70–77, <https://doi.org/10.1055/a-1031-7283>.
- [17] N. Ding, Y. Jiang, L. Han, X. Chen, J. Ma, X.D. Qu, Y. Mu, J. Liu, L.Y. Li, C.L. Jiang, X.S. Huang, Bafilomycins and odoriferous sesquiterpenoids from *Streptomyces albolongus* isolated from *elephas maximus* feces, *J. Nat. Prod.* 79 (4) (2016) 799–805, <https://doi.org/10.1021/acs.jnatprod.5b00827>.
- [18] P. Liu, Z. Yao, W. Zhang, Y. Takaishi, H.Q. Duan, Novel nortriterpenes from *Phlomis umbrosa*, *Chem. Pharm. Bull.* 56 (7) (2008) 951–955, <https://doi.org/10.1248/cpb.56.951>.
- [19] M. Ye, J. Xiong, J.J. Zhu, J.L. Hong, Y. Zhao, H. Fan, G.X. Yang, G. Xia, J.F. Hu, Leonurusoleanolides E–J, minor spirocyclic triterpenoids from *Leonurus japonicus* fruits, *J. Nat. Prod.* 77 (1) (2014) 178–182, <https://doi.org/10.1021/np400838a>.
- [20] I. Calis, H. Kirmizibekmez, D. Tasdemir, P. Ruedi, Two new triterpene and a new nortriterpene glycosides from *Phlomis viscosa*, *Helv. Chim. Acta* 87 (3) (2004) 611–619, <https://doi.org/10.1002/hlca.200490059>.
- [21] L. Di Bari, G. Pescitelli, C. Pratelli, D. Pini, P. Salvadori, Determination of absolute configuration of acyclic 1,2-diols with Mo-2(OAc)(4). 1. Snatzke's method revisited, *J. Org. Chem.* 66 (14) (2001) 4819–4825, <https://doi.org/10.1021/jo010136v>.
- [22] H.R. Wu, X.F. He, X.J. Jin, H. Pan, Z.N. Shi, D.D. Xu, X.J. Yao, Y. Zhu, New nor-ursane type triterpenoids from *Gelsemium elegans*, *Fitoterapia* 106 (2015) 175–183, <https://doi.org/10.1016/j.fitote.2015.09.002>.
- [23] J.C. Shu, J.Q. Liu, G.X. Chou, Z.T. Wang, Two new triterpenoids from *Psidium guajava*, *Chin. Chem. Lett.* 23 (7) (2012) 827–830, <https://doi.org/10.1016/j.ccllet.2012.05.018>.
- [24] P.K. Agrawal, NMR Spectroscopy in the structural elucidation of oligosaccharides and glycosides, *Phytochemistry* 31 (10) (1992) 3307–3330 [https://doi.org/https://doi.org/10.1016/0031-9422\(92\)83678-R](https://doi.org/https://doi.org/10.1016/0031-9422(92)83678-R).
- [25] H.J. Yuk, Y.S. Lee, H.W. Ryu, S.H. Kim, D.S. Kim, Effects of *Toona sinensis* leaf extract and its chemical constituents on xanthine oxidase activity and serum uric acid levels in potassium oxonate-induced hyperuricemic rats, *Molecules* 23 (12) (2018) 3254, <https://doi.org/10.3390/molecules23123254>.
- [26] M.N. Samy, S. Sugimoto, K. Matsunami, H. Otsuka, M.S. Kamel, One new flavonoid xyloside and one new natural triterpene rhamnoside from the leaves of *Syzygium grande*, *Phytochem. Lett.* 10 (2014) 86–90, <https://doi.org/10.1016/j.phytol.2014.08.009>.
- [27] A.S.R. Anjaneyulu, K.S. Sagar, M. Venugopal, Terpenoid and steroid constituents of the indian-ocean soft coral *Sinularia maxima*, *Tetrahedron* 51 (40) (1995) 10997–11010, [https://doi.org/10.1016/0040-4020\(95\)00655-r](https://doi.org/10.1016/0040-4020(95)00655-r).
- [28] M. Keusgen, M. Falk, J.A. Walter, K.W. Glombitza, A phloroglucinol derivative from the brown alga *Sargassum spinuligerum*, *Phytochemistry* 46 (2) (1997) 341–345, [https://doi.org/10.1016/S0031-9422\(97\)00277-X](https://doi.org/10.1016/S0031-9422(97)00277-X).
- [29] S.A. Belapure, Z.G. Beamer, J.E. Bartmess, S.R. Campagna, A biomimetic synthesis of (-)-ascorbyl phloroglucinol and studies toward the construction of ascorbyl-modified catechin natural products and analogues, *Tetrahedron* 67 (48) (2011) 9265–9272, <https://doi.org/10.1016/j.tet.2011.09.102>.
- [30] M. Nakai, Y. Fukui, S. Asami, Y. Toyoda-Ono, T. Iwashita, H. Shibata, T. Mitsunaga, F. Hashimoto, Y. Kiso, Inhibitory effects of oolong tea polyphenols on pancreatic lipase in vitro, *J. Agric. Food Chem.* 53 (11) (2005) 4593–4598, <https://doi.org/10.1021/jf047814+>.
- [31] Y. Zhu, Y. Zhao, P. Wang, M. Ahmedna, C.T. Ho, S. Sang, Tea Flavonols Block Advanced glycation of lens crystallins induced by dehydroascorbic acid, *Chem. Res. Toxicol.* 28 (1) (2015) 135–143, <https://doi.org/10.1021/tx500430z>.
- [32] P.Y. Chung, Novel targets of pentacyclic triterpenoids in *Staphylococcus aureus*: A systematic review, *Phytomedicine* 73 (2020) 152933, <https://doi.org/10.1016/j.phymed.2019.152933>.
- [33] B. Kim, J.W. Han, M.T. Ngo, Q.L. Dang, J.C. Kim, H. Kim, G.J. Choi, Identification of novel compounds, oleanane- and ursane-type triterpene glycosides, from *Trevesia palmata*: their biocontrol activity against phytopathogenic fungi, *Sci. Rep.* 8 (2018) 14522, <https://doi.org/10.1038/s41598-018-32956-4>.
- [34] C.M. Wang, Y.L. Jhan, S.J. Tsai, C.H. Chou, The Pleiotropic antibacterial mechanisms of ursolic acid against methicillin-resistant *Staphylococcus aureus* (MRSA), *Molecules* 21 (7) (2016) 884, <https://doi.org/10.3390/molecules21070884>.
- [35] L.R. Huang, H. Luo, Q.J. Li, D.P. Wang, J.X. Zhang, X.J. Hao, X.S. Yang, Pentacyclic triterpene derivatives possessing polyhydroxyl ring A inhibit Gram-positive bacteria growth by regulating metabolism and virulence genes expression, *Eur. J. Med. Chem.* 95 (2015) 64–75, <https://doi.org/10.1016/j.ejmech.2015.01.015>.
- [36] S. Mlala, A.O. Oyedeji, M. Gondwe, O.O. Oyedeji, Ursolic acid and its derivatives as bioactive agents, *Molecules* 24 (15) (2019) 2751, <https://doi.org/10.3390/molecules24152751>.
- [37] L.C.S. Cunha, M. Silva, N. Furtado, A.H.C. Vinholis, C.H.G. Martins, A.A. da Silva, W.R. Cunha, Antibacterial activity of triterpene acids and semi-synthetic derivatives against oral pathogens, *Z.Naturforsch. C* 62(9–10) (2007) 668–672, <https://doi.org/10.1515/znc-2007-9-1007>.
- [38] W. Gu, Y. Hao, G. Zhang, S.F. Wang, T.T. Miao, K.P. Zhang, Synthesis, *in vitro* antimicrobial and cytotoxic activities of new carbazole derivatives of ursolic acid, *Bioorg. Med. Chem. Lett.* 25 (3) (2015) 554–557, <https://doi.org/10.1016/j.bmcl.2014.12.021>.
- [39] I.P. Singh, J. Sidana, P. Bansal, W.J. Foley, Phloroglucinol compounds of therapeutic interest: global patent and technology status, *Expert Opin. Ther. Patents* 19 (6) (2009) 847–866, <https://doi.org/10.1517/13543770902916614>.
- [40] H. Bridi, G.V. Ccana-Ccapatinta, E.D. Stolz, G.C. Meirelles, S.A.L. Bordignon, S.M.K. Rates, G.L. von Poser, Dimeric acylphloroglucinols from *Hypericum austrobrasilense* exhibiting antinociceptive activity in mice, *Phytochemistry* 122 (2016) 178–183, <https://doi.org/10.1016/j.phytochem.2015.12.012>.
- [41] A.C. Stein, A.F. Viana, L.G. Muller, J.M. Nunes, E.D. Stolz, J.C. Do Rego, J. Costentin, G.L. von Poser, S.M.K. Rates, Uliginosin B, a phloroglucinol derivative from *Hypericum polyanthemum*: A promising new molecular pattern for the development of antidepressant drugs, *Behav. Brain Res.* 228 (1) (2012) 66–73, <https://doi.org/10.1016/j.bbr.2011.11.031>.